Thin Solid Films 689 (2019) 137502

Contents lists available at ScienceDirect

Thin Solid Films

journal homepage: www.elsevier.com/locate/tsf

Synthesis and optical properties of Ga_2O_3 nanowires grown on GaS substrate

Liviu Leontie[a,*], Veaceslav Sprincean[b], Dumitru Untila[b,c], Nicolae Spalatu[d], Iuliana Caraman[c], Ala Cojocaru[e,f], Oana Șușu[a], Oleg Lupan[f,g], Igor Evtodiev[b,c], Elmira Vatavu[b], Ion Tiginyanu[c,g], Aurelian Carlescu[h], Mihail Caraman[b]

[a] Faculty of Physics, Alexandru Ioan Cuza University of Iasi, Bulevardul Carol I, Nr. 11, RO-700506 Iasi, Romania
[b] Laboratory of Scientific Research "Photonics and Physical Metrology", Faculty of Physics and Engineering, Moldova State University, A. Mateevici, 60, MD-2009 Chisinau, Republic of Moldova
[c] Ghitu Institute of Electronic Engineering and Nanotechnologies, Academy of Sciences of Moldova, Academiei, 3/3, MD-2028 Chisinau, Republic of Moldova
[d] Tallinn University of Technology, Department of Materials Science, Ehitajate tee, 5, EE-19086 Tallinn, Estonia
[e] PhI-Stone AG, Kaiserstasse 2, D-24143 Kiel, Germany
[f] Functional Nanomaterials, Institute for Materials Science, Kiel University, Kaiser Str. 2, D-24143 Kiel, Germany
[g] Department of Microelectronics and Biomedical Engineering, Technical University of Moldova, Stefan cel Mare si Sfint bd., 168, MD-2004 Chisinau, Republic of Moldova
[h] Integrated Center for Studies in Environmental Science for North-East Region, Alexandru Ioan Cuza University of Iasi, Iasi 7000506, Romania

ARTICLE INFO

Keywords:
Gallium(III) trioxide
Gallium(III) sulfide
Thermal treatment
Oxidation
Structural properties
Optical properties
Photoluminescence

ABSTRACT

Gallium oxide (β-Ga_2O_3) nanowires were synthesized by heat treatment of single crystal β-GaS plates in air. Crystal structure and composition of synthesized materials were studied by X-ray diffraction, energy dispersive X-ray spectroscopy and Raman spectroscopy. Thermal treatment of β-GaS plates at 1023 K leads to the formation of a Ga_2O_3 (native oxide) layer on β-GaS (0001) surface of plates. Layer thickness and size of Ga_2O_3 wires contained were found to depend on temperature and duration of applied heat treatment. For 1023 K and 6 h, the length of Ga_2O_3 wires laid in the range from units to tens of nanometers, while for 1123 K and 30 min, between 30 and 40 μm.

1. Introduction

Nowadays, particular attention is paid to the improvement of preparation methods of oxide-semiconductor nanostructures due to their unique optical, photoelectric and photocatalytic properties [1–3]. Among other gallium oxide polymorphs, β-Ga_2O_3 has been extensively studied in recent years; displaying a monoclinic crystal structure with lattice parameters $a = 12.23$ Å, $b = 3.04$ Å, $c = 5.80$ Å, $\alpha = \gamma = 90°$ and $\beta = 103.7°$ [4], it is a *n*-type semiconductor with an energy band gap of 4.2–4.9 eV at room temperature [5–7]. This oxide semiconductor shows promise for diverse applications, including beam emitters at room temperature [8], optically transparent electrodes in solar cells and high temperature gas sensors [9].

Gallium oxide nanostructures with different surface morphologies and crystalline forms and sizes were obtained by various techniques, such as chemical vapor deposition (CVD) [10], thermal vacuum evaporation [11], as well as air quenching of GaN powder [12], and GaSe [4,13–15] and GaS [16,17] single crystals. Different structures with morphologies depending on the vapor temperature have been obtained by oxidation of Ga vapors in an Ar—O_2 atmosphere. In the vapor temperature range between 1150 K and 1273 K, nanostructures displaying morphologies from dispersed crystallites to microplates have been obtained [18]. In works [19–21] single crystalline α-Ga_2O_3 layers on Al_2O_3 substrates were obtained by CVD technique. From the polarized Raman scattering spectra the wavenumbers and symmetry of normal vibration modes characteristic of α-Ga_2O_3 single crystals were determined.

Gallium sulfide (GaS) displays a typical layered structure, each layer being composed of elementary Chalcogen-Metal-Metal-Chalcogen (S-Ga-Ga-S) stratified packings. Besides, own to the atomic arrangement within the crystal lattice, valence bonds of chalcogen atoms at (0001) surfaces are almost completely compensated. Due to its specific structural features, GaS is a promising material for semiconductor heterojunctions with various crystal structures [22–25].

In this work, micrometer-sized (20–50 μm) Ga_2O_3 films, composed of nanowires, are studied. These were obtained by thermal oxidation of GaS plates with the same thickness, in normal atmosphere.

The morphology, type of nano-formations and photoluminescence (PL) spectra of nanowires have been investigated using Scanning Electron Microscopy (SEM) analysis, Raman scattering spectroscopy

* Corresponding author.
E-mail address: lleontie@uaic.ro (L. Leontie).

https://doi.org/10.1016/j.tsf.2019.137502
Received 7 January 2019; Received in revised form 14 August 2019; Accepted 14 August 2019
Available online 16 August 2019
0040-6090/

and powder X-ray diffraction (XRD) technique. For comparison purposes, similar studies of single crystal β-GaS plates prepared by Bridgman technique from elemental components were presented.

2. Sample preparation

Gallium sulfide (β-GaS) single crystals were grown by Bridgman-Stockbarger technique using the synthesized compound as the primary material. The GaS with a mass of 20 g was synthesized from Ga (5 N) and S (5 N) elements taken in stoichiometric proportions. The respective amounts of Ga and S were introduced into quartz ampoules with an internal diameter of ~14 mm and graphite-coated inner walls of ~20 cm length. After pumping down the ampoules to the residual gas pressure of 6.67×10^{-3} Pa, they were sealed and placed in a two-zone (zone I and zone II) furnace, tilted at 30 degrees towards the horizontal. Initially, the elements were placed in the second section of the oven, so that ~1/3 of the length of the ampoule remained outside the furnace. The temperature in the second sector was slowly increased to 1323 k for 6 h. During this time, the ampoule rotated at ~2 rpm. The amount of condensed sulfur in the cold portion of the ampoule decreased gradually, eventually leading to the formation of GaS. The overall synthesis process took 10–12 h. Thereafter the ampoule was gradually introduced into the furnace, so that the temperature of 1323 K was set over the entire length of the ampoule, after which the furnace was moved vertically. In zone I of the furnace the temperature was set to ~1173 K. Further, the molten substance was proceeded through a temperature gradient (zone II) with a speed of ~ 1 mm/h. After that, the temperature in sectors I and II was decreased to room temperature at a rate of 150 K/h. In this way, single crystal ingots were obtained that easily split along the cleavage planes. By splitting bulk single crystalline ingots perpendicularly to the C_6 axis, plan-parallel plates, atomically smooth and optically homogeneous were obtained, with thickness in the range of 20–200 μm. These were further subjected to a heat treatment in air, at temperatures of 1023–1223 K, with the durations from 30 min to 6 h.

As a result of heat treating, the surface of GaS plate is covered with a white thick layer, the thickness of which increases with heat treatment duration. After thermal treatment in normal atmosphere, at 1150 K, the GaS plates with thickness of 20–50 μm turned into oxide over their entire thickness. These were further selected as samples in actual investigations.

The oxide layer displays a granular (rough) shape, which is likely to produce diffuse reflection of incident light. Surface morphology of samples was studied using SEM micrographs, recorded with a Zeiss Ultra Plus electron microscope (7 kV, 10 μA), equipped with an EDX (energy dispersive X-ray spectroscopy) analysis system [a Si/Li detector (Noran, Vantage System)]. The crystal structure of GaS-Ga_2O_3 composite was studied by XRD technique in the angular range between 20° and 90° with a Rigaku Ultima IV diffractometer (CuK_α radiation, $\lambda = 1.5406$ Å, 40 kV and 40 mA, D/teX Ultra detector), in Bragg-Brentano (θ–2θ) geometry. Raman scattering spectra at room temperature were recorded in a backward configuration (180°) with a Raman spectrometer of WITec alpha300 R type, using exciting radiation of an Ar^+ ion laser (wavelength $\lambda = 514.5$ nm, power of ~2 mW). Photoluminescence of GaS-Ga_2O_3 composite was excited with the 253 nm wavelength radiation provided by a DRS-250 Hg vapor lamp. Respective wavelength was selected using a quartz prism monochromator. The emission spectrum was recorded using a photometric equipment including a MDR-2 monochromator with diffraction gratings (600 and 1200 mm^{-1}). The emitted radiation was recorded by means of a photomultiplier with $Na_2KSb(Cs)$ photocatode with quartz window.

3. Results and discussion

3.1. XRD structural analysis

Crystal structure determination and phase identification in the case of β-GaS plates, heat treated in air, was performed using XRD diagrams. Curve 1 (Fig. 1) shows the XRD pattern of GaS plate prior to heat treatment. The provided pattern emphasizes presence of intense diffraction lines at 2θ angles of 22.98°, 11.46° and 34.74°, corresponding to (004), (002) and (006) atomic planes of hexagonal β-GaS (PDF 01-071-0009 file), respectively, with lattice constants $a = 3.587$ Å and $c = 15.498$ Å.

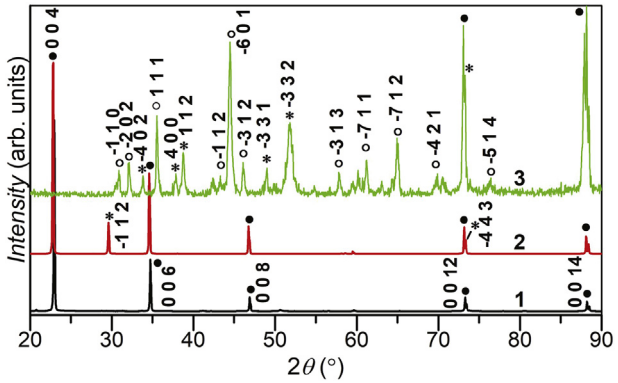

Fig. 1. Powder XRD patterns of GaS samples prior to (curve 1) and after heat treatment in air, for 6 h, at 1023 K (curve 2) and at 1123 K (curve 3) (● β-GaS, PDF 01-071-0009; * Ga_2S_3, PDF 01-071-2672; ○ Ga2O3, PDF00-041-1103).

As a result of heat treating of GaS single crystals at 1023 K for 6 h, the sample surface becomes white-red. The XRD pattern of respective samples (Fig. 1, curve 2) contains characteristic GaS lines, together with an intense diffraction line at $2\theta = 29.60°$, identified as (112) reflection (card PDF 01–071-2672) of hexagonal Ga_2S_3, as well as, a few low intensity lines in the 2θ range between 20° and 90°. The intensity of these lines does not exceeds 0.2% of that of (004) line (highest peak intensity) of hexagonal GaS. According to PDF 01-071-2672 and 00-041-1103 cards, these lines can be identified as diffraction lines of hexagonal Ga_2S_3 and traces of monoclinic β-Ga_2O_3 phase. Thus, at 1023 K, GaS → Ga_2S_3 phase transition occurs and structural transformation GaS → Ga_2O_3 is initiated. The phase transition is an intermediate one in the GaS → Ga_2S_3 → Ga_2O_3 chain. As mentioned in [26], an analogous transformation is possible upon thermal oxidation of GaSe films with formation of Ga_2O_3. Temperature increase from 1023 K to 1123 K results in attenuation of > 100 times the intensity of characteristic XRD lines of hexagonal GaS and at the same time, formation of new diffraction lines (Fig. 1, curve 3). The XRD pattern of the sample obtained by heat treatment at 1173 K for 0.5 h is similar to that shown in Fig. 1, curve 3.

The XRD pattern of GaS samples subjected to heat treatment at 1123 K for 6 h (Fig. 1, curve 3) contains traces of hexagonal β-GaS and a series of intense XRD lines, that, according to PDF 00–041-1103 card, can be ascribed to monoclinic β-Ga_2O_3 phase with lattice parameters $a = 12.23$ Å, $b = 3.04$ Å, $c = 5.50$ Å and $\beta = 103.7°$ [27]. As can be inferred from Fig. 1, curve 1, the highest intensity diffraction lines are due to lattice planes predominantly oriented parallel to the C_6 axis of GaS single crystals. The composite obtained by heat treatment at 1123 K contains monoclinic β-Ga_2O_3 single crystals, with lattice constants $a = 1.22$ nm, $b = 0.31$ nm, $c = 0.58$ nm and $\beta = 103.7°$.

Along with the XRD lines of β-Ga_2O_3 nano-formations, a series of low-intensity lines and widened contours is also emphasized. These lines indicate the presence of nanocrystalline Ga_2S_3 in the composite (PDF 01-071-2672 card). The occurrence of this phase confirms the assumption [27] that at high temperatures, in the presence of oxygen, hexagonal Ga_2S_3 phase is initially formed, which eventually yields nanosized β-Ga_2O_3 as a result of the sulfur substitution by oxygen.

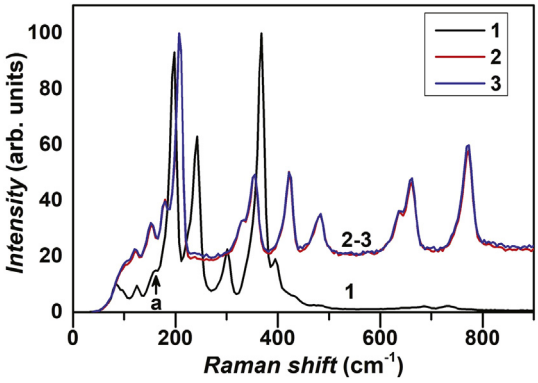

Fig. 2. Raman spectra of composites obtained by thermal treatment of GaS plates in air, at 1023 K for 6 h (curve 1), 1123 K, for 6 h (curve 2-blue color) and 1173 K, for 30 min (curve 3-red color). (For interpretation of the references to color in this figure legend, the reader is referred to the web version of this article.)

3.2. Raman structural analysis

The structure of the as obtained material was also investigated using Raman scattering spectroscopy (Fig. 2). Gallium sulfide (β-GaS) is a hexagonal layered single crystal and belongs to the space group D_{6h}^3. For this group, the irreducible representations of the vibration modes in the center of the Brillouin zone ($\vec{\kappa} = 0$) are $2(A_{1g} + A_{2u} + B_{1u} + B_{2g} + E_{1g} + E_{1u} + E_{2g} + E_{2u})$. Among these, A_{1g} and E_{2g} are Raman active modes in respective spectra. The well-known Raman scattering spectrum of β-GaS crystals, lying between 50 and 400 cm^{-1}, comprises typical vibration modes at 74.2 cm^{-1} (E_{1g}^1), 188.0 cm^{-1} (A_{1g}^1), 291.4 cm^{-1} (E_{1g}^2), 295.2 cm^{-1} (E_{2g}^1) and 359.9 cm^{-1} (A_{1g}^2) [28].

In turn, β-Ga_2O_3, with monoclinic crystal structure, belongs to the $C_{2/m}$ space group [29]. There are 15 vibration modes in the Raman spectrum of this compound. In Fig. 2, curve 1, the Raman spectrum of the sample obtained by heat treatment of GaS plate in air, at 1023 K for 6 h is presented. As can be observed, it also contains, along with the vibration modes of hexagonal β-GaS lattice, four bands with maxima located at 115.7 cm^{-1}, 152.2 cm^{-1}, 233.9 cm^{-1} and 386.1 cm^{-1}. The increase in the heat treatment temperature from 1023 K to 1123 K substantially alters the shape of the Raman spectrum (Fig. 2, curve 2). So, the background level of the Raman lines corresponding to the vibration modes of β-GaS (hexagonal lattice) are seen to attenuate. In this spectrum, the line at 359.4 cm^{-1} is the only emphasized. As can be seen from Fig. 2, the Raman spectrum of the composite obtained by heat treatment of GaS plate at 1173 K for 30 min (curve 3) is identical to that obtained for 6 h heat treatment at 1123 K (curve 2).

In Table 1 the wavenumbers of the Raman active vibration modes (Fig. 2) of the samples are listed. The respective Raman lines were interpreted using comparisons with the Raman spectra (vibration modes) of β-GaS, β-Ga_2S_3 and β-Ga_2O_3. As it can be seen from this table, heat treatment in air at 1023 K for 6 h leads to phase transformation of initial β-GaS in β-Ga_2S_3. The presence of the "*a*" threshold at 152 cm^{-1} (Fig. 2) indicates that the formation of β-Ga_2O_3 single crystal occurs at this temperature. The Raman spectrum of the sample synthesized at 1123 K does not contain Raman lines characteristic of the vibration modes of hexagonal β-GaS. Therefore, at this temperature crystallites composed of β-Ga_2S_3 and β-Ga_2O_3 are formed, as confirmed by the XRD diagrams. The wide contour of the XRD lines attests the nanometric sizes of Ga_2S_3 and Ga_2O_3 single crystals in the studied composite.

The similarity of the Raman spectra of samples synthesized at 1123 K for 6 h and 1173 K for 30 min indicates the rapidity of the GaS oxidation at temperatures near the melting point of the compound. The relative low intensity of Raman lines at 114 cm^{-1}, 146 cm^{-1} and 324 cm^{-1} can serve as an indicator that at 1123 K and above an oxidation reaction predominates, as proposed in [27]:

$$4\ GaS + 3\ O_2 \rightarrow 2\ Ga_2O_3 + 2\ S_2$$

Table 1
Interpretation of the Raman spectra of composites obtained by heat treatment of GaS plates in air.

No.	GaS heat treated in air			β-GaS [29]	β-Ga_2S_3 [30]	β-Ga_2O_3 [18,31]	Identification
	1023 K	1123 K	1173 K				
	6 h	6 h	0.5 h				
1	74.4			74	72		β-GaS
2	96.0				98		β-Ga_2S_3
3	115.7	114	114		114	117.60	β-Ga_2S_3
4	–	146	146		146	147.53	β-Ga_2S_3
5	152.2						
6		173.4	174			172.92	β-Ga_2O_3
7	188.6			188			β-GaS
8		201.0	201.2			202.60	β-Ga_2O_3
9	233.9				233		β-Ga_2S_3
10	292.4			292	280		β-GaS
11			322	318	321	322.13	β-Ga_2S_3
							β-Ga_2O_3
12		326.8			329		β-Ga_2S_3
13		349.1	349.1		343	348.98	β-Ga_2O_3
14	359.4			361	368		β-GaS
15	386.1				386		β-GaS
16		416	416		404	418.27	β-Ga_2O_3
17		474	477.5			477.36	β-Ga_2O_3
18		630	630			630.78	β-Ga_2O_3
19		655.9	656			654.31	β-Ga_2O_3
20		767.2	767.3			768.41	β-Ga_2O_3

3.3. SEM morphological analysis

The surface morphology of the composite synthesized by heat treatment of β-GaS plates in air, at 1023 K, 1123 K and 1173 K was studied using SEM micrographs (Fig. 3). As can be seen from Fig. 3a, as a result of heat treatment at 1023 K, the GaS (0001) surface of the plate is coated with a homogeneous composite layer. The X-ray diffractograms (Fig. 1) shows that this composite consists of GaS and Ga_2S_3 single crystals, as well as small amounts of β-Ga_2O_3 native oxide. So, it is confirmed that at 1023 K, in the presence of oxygen, phase transformation of GaS in Ga_2S_3 takes place. When increasing the heat treatment temperature from 1023 K to 1123 K, as shown in Fig. 3b, the (0001) surface of β-GaS plate is covered with a layer composed of needle-shaped micro-formations and chaotically oriented ribbons. The average length of these formations is ~3 μm, while the width of the ribbons does not exceed 0.5 μm.

When increasing the heat treatment temperature to 1173 K and decreasing ~10 times its duration, it can be observed that the ribbon length increases on average about 1.5–2.0 times. At the same time, their width also increases proportionally. Under these synthesis conditions, formation of 15–20 μm length wires takes place. Their amount, determined by statistical analysis of SEM images, is about 10%. Along with multitude of needles and chaotically oriented ribbons on the surface of samples synthesized at 1123 K, some truncated cone shapes can be also observed on the surface at 1173 K (Fig. 3c), which play the role of growth centers for Ga_2O_3 nanoneedles.

Several technologies have been developed for the fabrication of β-Ga_2O_3 layers containing nano-formations. A brief characterization of the most widespread methods can be found in [32]. In work [7], β-Ga_2O_3 nano-formations were obtained from Ga vapor phase, in a Ar—O (50:5) atmosphere. It has been established that the type of formations depends on the synthesis temperature of gallium oxide. Thus, at 1150 K, β-Ga_2O_3 micrograins are formed on sapphire substrate, while microplates and nanowires are formed at temperatures of 1250 K and 1270 K,

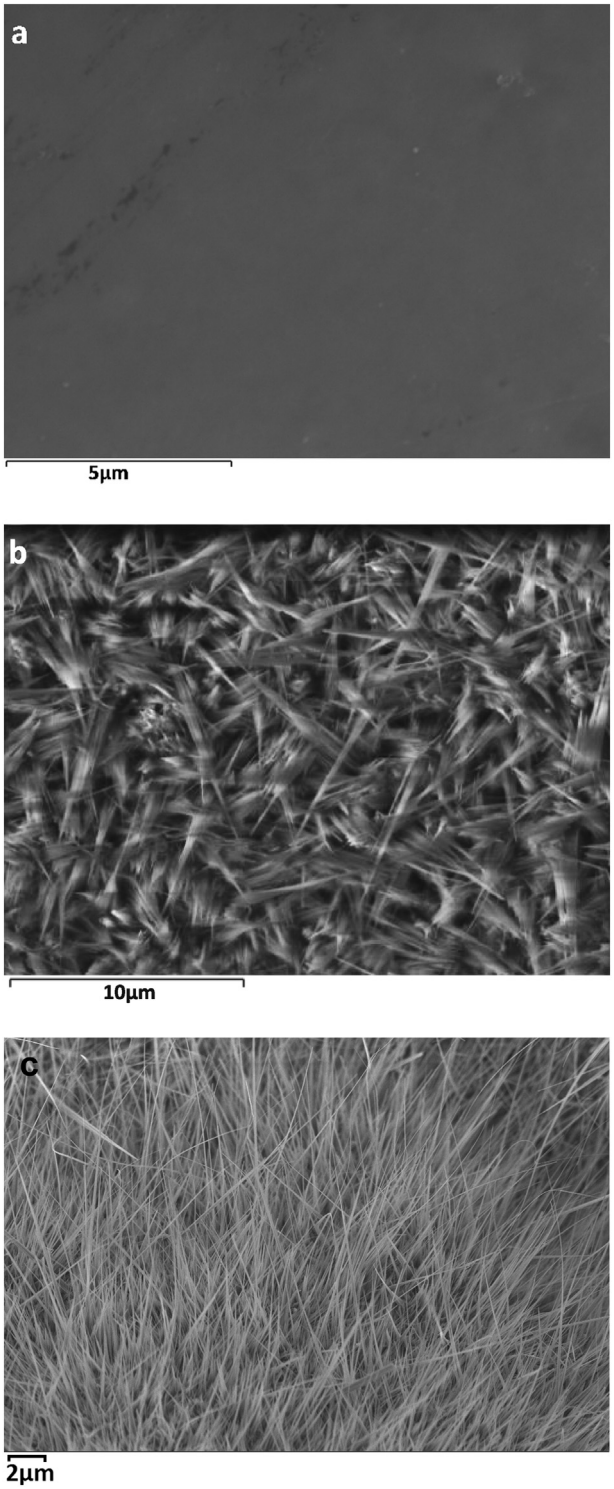

Fig. 3. SEM images of the composite surface of GaS plates heat treated in air, at 1023 K for 6 h (a), 1123 K for 6 h (b) and 1173 K for 30 min (c).

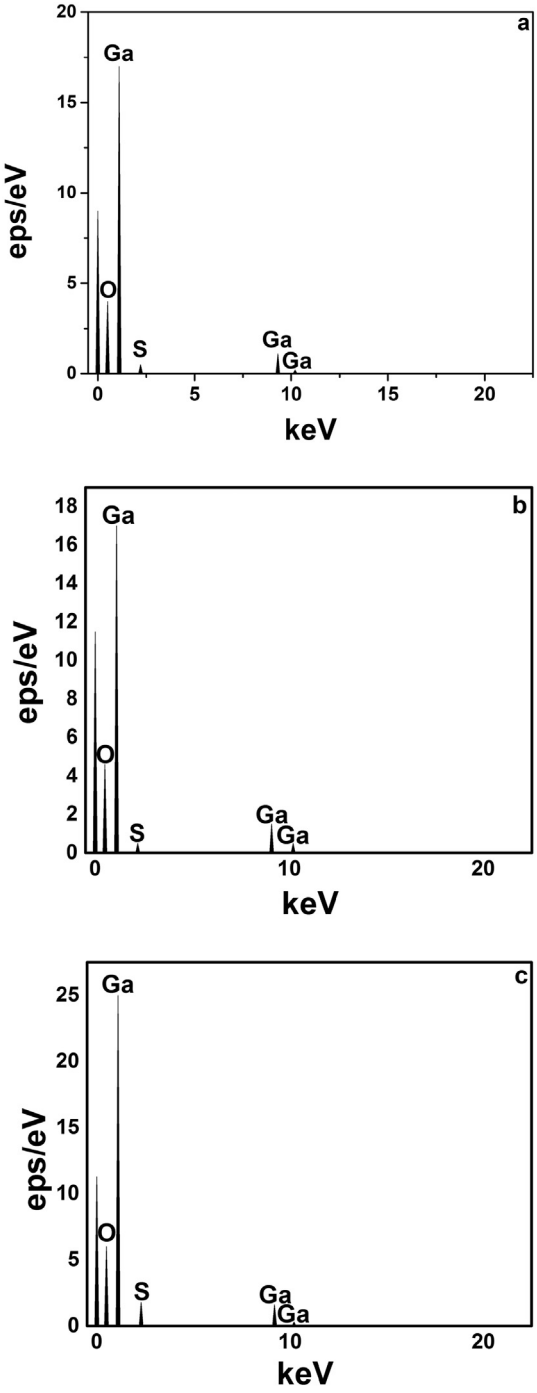

Fig. 4. The elemental analysis of the composite obtained after heat treatment of GaS plates in air, at 1023 K for 6 h (a), 1123 K for 6 h (b) and 1173 K for 30 min (c).

respectively. Submicrometer length β-Ga_2O_3 nonocones were obtained by heat treatment of GaS lamellas in H_2O vapors [17]. Besides, β-Ga_2O_3 nanowires with average lengths of 4–10 μm were obtained by heat treatment of GaSe lamellas in a Ar-air atmosphere, at temperature of 1200 K [4].

3.4. EDX compositional analysis

As can be seen from the analysis of the XRD diagrams and Raman scattering spectra, heat treatment of the GaS plate at 1023 K for 6 h leads to the formation of a material composed of GaS (base material), β-Ga_2S_3 phase and a small amount of Ga_2O_3. The elemental composition of the formations present on the sample surface was analyzed by the EDX technique (Fig. 4). From Fig. 4a, it can be seen clearly that on an arbitrarily selected area the element concentration are 58 at. % oxygen, 39 at. % gallium and 3 at. % sulfur. The variation of these amounts from one surface area to another is ~10%.

The EDX diagram of the composite formed at 1123 K is shown in Fig. 4b. From this figure it can be seen that by increasing the heat treatment temperature by 100 K (from 1023 K to 1123 K), sulfur is only

found as traces on the sample surface. The concentration of Ga atoms increased from 39 at. % (at 1023 K) to 43 at. % in the composite obtained at 1123 K. These samples show a decrease in oxygen concentration of ~1–2 at. %.

The EDX diagram of a selected arbitrary element of the synthesized sample at 1173 K, shown in Fig. 4c, attests the presence of Ga and O atoms with a concentration of 56 at. % and 44 at. %, respectively. Thus, heat treatment of ~100 μm thick GaS plates in the air, at 1173 K for 30 min, leads to the formation of β-Ga_2O_3 with a small excess of oxygen. We mention that as a result of the thermal treatment of gallium nitride (GaN), at 1073 K, in normal atmosphere, on both lateral surface and interior of the sample, submicrometer-sized β-Ga_2O_3 particles were formed, with a composition close to the stoichiometric one (2:3) [33]. It is known that β-Ga_2O_3, in the form of nanowires, nanorods and nanoparticles, is an effective gas absorber/adsorber [9]. So, the emphasized surplus amount of oxygen could be due to oxygen adsorbed from the atmosphere over the time interval from material synthesis until measurements are carried out.

As can be seen from Fig. 1 curve 3, the material obtained by annealing of GaS plates, at 1173 K, for 0.5 h, also contains GaS and Ga_2S_3 crystallites. The low concentration of sulfur (< 0.1 at. %) in the samples obtained under these conditions attests the low concentration of respective (GaS and Ga_2S_3) crystallites in studied samples.

3.5. Photoluminescent properties

The fundamental absorption edge of nanosized Ga_2O_3 contains two regions of decreased absorption: one with a rapid decrease in the region of 250–270 nm and the other with a slow absorption decrease over the wavelength range of 270–355 nm [27]. The photoluminescence spectra of the composite obtained by heat treatment of GaS plate in air, at 1123 K for 6 h (Fig. 5a), were recorded at room temperature, with an exciting radiation wavelength of 253 nm (4.90 eV) corresponding to the first intense absorption range, and 337.4 nm (3.67 eV-a He—N_2 laser used in pulse mode), for the weaker absorption range.

Upon PL excitation at 253 nm, the emission spectrum covers the wavelength range from 350 nm to ~550 nm. As can be seen from Fig. 5a (curve 1), the PL contour can be properly decomposed into three Gaussian curves with maxima at 390 nm (a), 418 nm (b) and 440 nm (c) wavelengths. The structure of this PL spectrum can be explained if one admits that in the forbidden energy gap of β-Ga_2O_3 nano-formations three energy levels are formed, one donor and two acceptors (with energies E_D and E_A' and E_A", respectively-Fig. 5b).

In works [34,35] it was shown that the oxygen (V_O) and gallium vacancies (V_{Ga}) engender a donor level with energy of 1.72 eV (relative to the bottom of conduction band) and an acceptor level, respectively, at ~ 0.30 eV above the top of the valence band [34,35]. Since the forbidden bandwidth of β-Ga_2O_3 nano-formations is equal to 4.9 eV [36], the PL band (a), located at 390 nm, with the energy position of 3.18 eV, can be interpreted as the recombination of electrons on the donor level with energy of 1.72 eV with holes from the valence band.

The PL bands (b) and (c), with maxima at 2.97 eV (418 nm) and 2.82 eV (440 nm), can be considered as recombination of electrons on the same donor level (with energy of 1.72 eV) with holes from the acceptor levels with energies of 0.21 eV and 0.36 eV, respectively. The energy level diagram of β-Ga_2O_3, obtained from the PL spectrum excited at a photon energy of 4.90 eV (Fig. 5a) is shown in Fig. 5b.

In Fig. 5a (curve 2), the PL spectrum of β-Ga_2O_3 nano-formations, at excitation photon energy of 3.67 eV is shown. The excitation flux density at this wavelength was ~ 1000 times higher than in the case of 4.90 eV photon energy (curve 1). As can be seen from the comparison of curves 1 and 2, upon decreasing excitation energy by ~ 1.3 eV, the PL particularities located at 390 nm and 418 nm (curve 1) turn into an increasing intensity continuum and a maximum located at 455 nm (2.72 eV) is emphasized. This band can be interpreted as electron-hole recombination in donor-acceptor pairs. Photoluminescence in this spectral region was also reported for β-Ga_2O_3 nanowires synthesized by CVD at 1273 K [37]. The visible PL spectrum of respective nanowire structures is interpreted as radiative annihilation of charge-transfer excitons.

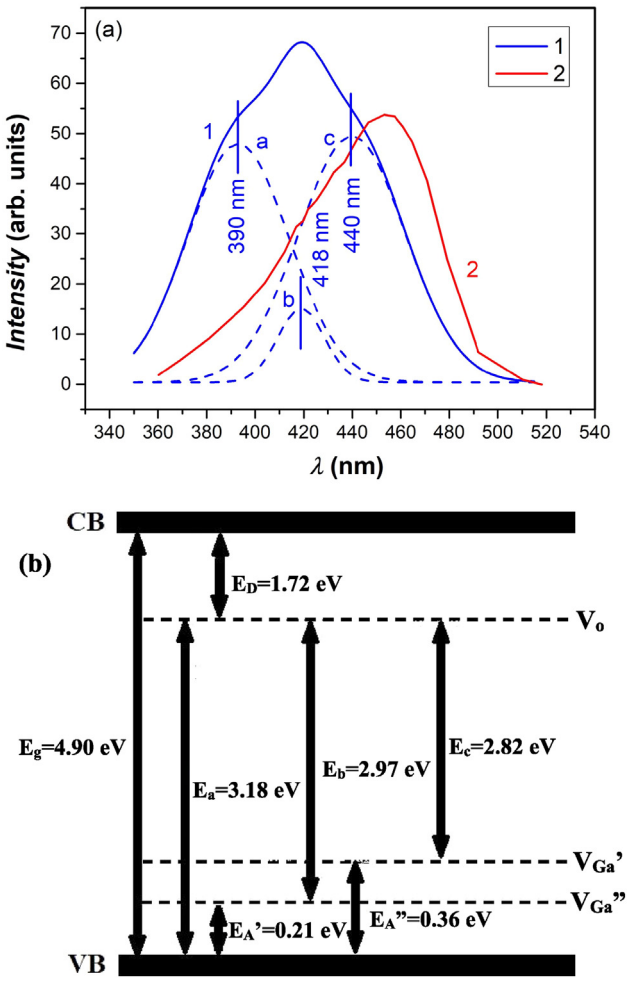

Fig. 5. (a) The PL spectra of the composite obtained by heat treatment of GaS plate in air, at 1123 K for 6 h, recorded at room temperature, at 253 nm (4.90 eV) (curve 1-blue color) and 337.4 nm (3.67 eV) (curve 2-red color) exciting wavelengths. Dashed curves: deconvolution of curve 1; (b) energy level diagram of β-Ga_2O_3. (For interpretation of the references to color in this figure legend, the reader is referred to the web version of this article.)

4. Conclusions

Gallium oxide (β-Ga_2O_3) nanowires and nanoribbons were obtained by thermal treatment of GaS plates in air at 1173 K. At 1123 K a crystalline composite composed of β-Ga_2O_3 and β-Ga_2S_3 is formed. By thermal treatment of GaS plates at 1023 K, a composite of GaS and Ga_2S_3 single crystals was obtained. The composition and crystal structure of the synthesized material at temperatures of 750–1173 K was determined by means of XRD, EDX analysis and Raman scattering spectra. The surface morphology of the synthesized composites was studied using SEM micrographs, from which it was determined that nano-formations synthesized at 1123 K are made of nanowires which converts into ribbons when the heat treatment temperature is increased to 1173 K. The composite of needles and chaotically oriented β-Ga_2O_3 ribbons on the sample surface is a broadband photoluminescent material in the visible range. The contour of the PL bands depends on the excitation energy. Reducing the excitation energy from 4.90 eV to 3.67 eV results in a PL peak redshift of ~40 nm.

Acknowledgements

This work was financially supported by Moldova State University through the Institutional Grant No. 15.817.02.34A, the Estonian Ministry of Education and Research (IUT19-4), as well as the European Regional Development Fund [project TK141: Centre of Excellence 'Advanced materials and high-technology devices for sustainable energetics, sensorics and nano-electronics' (1.01.2015–1.03.2023)]. Doctor Lupan gratefully acknowledges the Alexander von Humboldt Foundation for the fellowship for experienced researchers at the University of Kiel, Germany.

References

[1] J. Gan, X. Lu, J. Wu, S. Xie, T. Zhai, M. Yu, Z. Zhang, Y. Mao, S.C.I. Wang, Y. Shen, Y. Tong, Oxygen vacancies promoting photoelectrochemical performance of In_2O_3 nanocubes, Sci. Rep. 3 (2013) 1021.

[2] K. Grossmann, U. Weimar, N. Barsan, Semiconducting metal oxides based gas sensors, in: E.R. Weber, C. Jagadish (Eds.), Semiconductors and Semimetals, vol. 88, Elsevier, Amsterdam, 2013, pp. 261–282.

[3] A. Tiwari, M. Syväjärvi, Advanced 2D Materials, John Wiley & Sons, Beverly, MA, USA, 2016.

[4] E. Filippo, M. Siciliano, A. Genga, G. Micocci, A. Tepore, T. Siciliano, Single crystalline β-Ga_2O_3 nanowires synthesized by thermal oxidation of GaSe layer, Mater. Res. Bull. 48 (5) (2013) 1741–1744.

[5] M. Orita, H. Ohta, M. Hirano, H. Hosono, Deep-ultraviolet transparent conductive β-Ga_2O_3 thin films, Appl. Phys. Lett. 77 (25) (2000) 4166–4168.

[6] H.H. Tippins, Optical absorption and photoconductivity in the band edge of $\beta-Ga_2O_3$, Phys. Rev. 140 (1A) (1965) A316–A319.

[7] Z. Chen, X. Wang, K. Saito, T. Tanaka, M. Nishio, Q. Guo, The impact of growth temperature on the structural and optical properties of catalyst-free β-Ga_2O_3 nanostructures, Mater. Res. Express 3 (2) (2016) (UNSP 025003).

[8] Y. Bayam, V.J. Logeeswaran, A.M. Katzenmeyer, R.B. Sadeghian, R.J. Chacon, M.C. Wong, C.E. Hunt, K. Motomiya, B. Jeyadevan, M.S. Islam, Synthesis of Ga_2O_3 nanorods with ultra-sharp tips for high-performance field emission devices, Sci. Adv. Mater. 7 (2015) 1–7.

[9] C. Baban, Y. Toyoda, M. Ogita, Oxygen sensor based on Ga_2O_3 films operating at high temperature, J. Optoelectron. Adv. Mater. 7 (2) (2005) 891–896.

[10] L. Cao, M.K. Li, Z. Yang, Q. Wei, W. Zhang, Synthesis and characterization of dentate-shaped β-Ga_2O_3 nano/microbelts via a simple method, App. Phys. A Mater. Sci. Process. 91 (3) (2008) 415–419.

[11] J. Zhang, F. Jiang, Catalytic growth of Ga_2O_3 nanowires by physical evaporation and their photoluminescence properties, Chem. Phys. 289 (2–3) (2003) 243–249.

[12] B.C. Kim, K.T. Sun, K.S. Park, K.J. Im, T. Noh, M.Y. Sung, S. Kim, S. Nahm, Y.N. Choi, S.S. Park, β-Ga_2O_3 nanowires synthesized from milled GaN powders, Appl. Phys. Lett. 80 (3) (2002) 479–481.

[13] E. Filippo, M. Tepore, F. Baldassarre, T. Siciliano, G. Micocci, G. Quarta, L. Calcagnile, A. Tepore, Synthesis of β-Ga_2O_3 microstructures with efficient photocatalytic activity by annealing of GaSe single crystal, Appl. Surf. Sci. 238 (2015) 69–74.

[14] H. Iwakuro, C. Tatsuyama, S. Ichimura, XPS and AES studies on the oxidation of layered semiconductor GaSe, Jpn. J. Appl. Phys. 21 (1) (1982) 94–99.

[15] T.E. Beechem, B.M. Kowalski, M.T. Brumbach, A.E. McDonald, C.D. Spataru, S.W. Howell, T. Ohta, J.A. Pask, N.G. Kalugin, Oxidation of ultrathin GaSe, Appl. Phys. Lett. 107 (17) (2015) 173103.

[16] O.A. Balitskii, V.P. Savchyn, V.O. Yukhymchuk, Raman investigation of InSe and GaSe single-crystals oxidation, Semicond. Sci. Technol. 17 (2) (2002) L1–L4.

[17] E. Filippo, T. Siciliano, A. Genga, G. Micocci, M. Siciliano, A. Tepore, Phase and morphological transformations of GaS single crystal surface by thermal treatment, Appl. Surf. Sci. 261 (2012) 454–457.

[18] Z. Chen, X. Wang, K. Saito, T. Tanaka, M. Nishio, Q. Guo, The impact of growth temperature on the structural and optical properties of catalyst-free β-Ga_2O_3 nanostructures, Mater. Res. Express 3 (2) (2016) (UNSP 025003).

[19] R. Cuscó, N. Domènech-Amador, T. Hatakeyama, T. Yamaguchi, T. Honda, L. Artús, Lattice dynamics of a mist-chemical vapor deposition-grown corundum-like Ga_2O_3 single crystal, J. Appl. Phys. 117 (18) (2015) 185706.

[20] D. Shinohara, S. Fujita, Heteroepitaxy of corundum-structured α-Ga_2O_3 thin films on α-Al_2O_3 substrates by ultrasonic mist chemical vapor deposition, Jpn. J. Appl. Phys. Part 1 47 (9) (2008) 7311–7313.

[21] K. Akaiwa, S. Fujita, Electrical conductive corundum-structured α-Ga_2O_3 thin films on sapphire with tin-doping grown by spray-assisted mist chemical vapor deposition, Jpn. J. Appl. Phys. 51 (7) (2012) 070203.

[22] C. Galvan, M. Galvan, J.S. Arias-Ceron, E. Lopez-Luna, H. Vilchis, V.M. Sanchez-R, Structural and Raman studies of Ga_2O_3 obtained on GaAs substrate, Mater. Sci. Semicon. Process. 41 (2016) 513–518.

[23] N. Okamoto, N. Hara, H. Tanaka, Surface passivation of InGaP/InGaAs/GaAs pseudomorphic HEMTs with ultrathin GaS film, IEEE Trans. Electron. Dev. 47 (12) (2000) 2284–2289.

[24] Z.R. Dai, S.R. Chegwidden, L.E. Rumaner, F.S. Ohuchi, Microstructure evolution of GaSe thin films grown on GaAs (100) by molecular beam epitaxy, J. Appl. Phys. 85 (5) (1999) 2603–2608.

[25] C. Tatsuyama, H. Nishiwaki, K. Asai, K.K. Lim, T. Tambo, H. Ueba, Substrate orientation dependence of the growth of GaSe thin films on GaAs, Appl. Surf. Sci. 117 (1997) 523–529.

[26] O.A. Balitskii, V.P. Savchyn, P.V. Savchyn, Thermal oxidation of indium and gallium sulphides, Phys. B Cond. Matt. 355 (1–4) (2005) 365–369.

[27] K. Girija, S. Thirumalairajan, D. Mangalaraj, Morphology controllable synthesis of parallely arranged single-crystalline β-Ga_2O_3 nanorods for photocatalytic and antimicrobial activities, Chem. Eng. J. 236 (2014) 181–190.

[28] J.P. van der Ziel, A.E. Meixner, H.M. Kasper, Raman scattering from β-GaS, Solid State Commun. 12 (11) (1973) 1213–1215.

[29] E. Finkman, A. Rizzo, Lattice vibrations and the crystal structure of GaS and GaSe, Solid State Commun. 15 (11 − 12) (1974) 1841–1845.

[30] G. Lucazeau, J. Leroy, Etude vibrationnelle de α-Ga_2S_3, Spectrochim. Acta Part A 34 (1) (1978) 29–32.

[31] F.K. Cai, S. Shen, C. Yan, S. Bateman, Preparation, characterization and formation mechanism of gallium oxide nanowires, Curr. Appl. Phys. 8 (3–4) (2008) 363–366.

[32] S. Kumar, R. Singh, Nanofunctional gallium oxide (Ga_2O_3) nanowires/nanostructures and their applications in nanodevices, Phys. Stat. Sol. (RRL)–Rapid Res. Lett. 7 (10) (2013) 781–792.

[33] H.-D. Xiao, H.-L. Ma, C.-S. Xue, et al., Synthesis and structural properties of beta-gallium oxide particles from gallium nitride powder, Mater. Chem. Phys. 101 (1) (2007) 99–102.

[34] E. Nogales, B. Méndez, J. Piqueras, Cathodoluminescence from β-Ga_2O_3 nanowires, Appl. Phys. Lett. 86 (2005) 86 (11) 113112.).

[35] F. Alema, B. Hertog, O. Ledyaev, et al., Solar blind photodetector based on epitaxial zinc doped Ga_2O_3 thin film, Phys. Status Solidi A 214 (5) (2017) 1600688.

[36] S. Cui, Z. Mei, Y. Zhang, et al., Room-temperature fabricated amorphous Ga_2O_3 high-response-speed solar-blind photodetector on rigid and flexible substrates, Adv. Opt. Mater. 5 (19) (2017) 1700454.

[37] Y. Li, T. Tokizono, M. Liao, et al., Efficient assembly of bridged β-Ga2O3 nanowires for solar-blind photodetection, Adv. Funct. Mater. 20 (22) (2010) 3972–3978.